2015 Progress Report (DE-SC000936) / July 2016

Michelle M. Scherer
University of Iowa

Iron Oxide Redox Transformation Pathways: The Bulk Electrical Conduction Mechanism

Kevin M. Rosso (PI: PNNL) and Michelle Scherer (CoPI: University of Iowa)

Project Background

Despite decades of research on the reactivity and stable isotope properties of Fe oxides, the ability to describe the redox behavior of Fe oxides in the environment is still quite limited. This is due, in large part, to the analytical and spatial complexities associated with studying microscopic processes at the Fe oxide-water interface. This project had the long-term vision of filling this gap by developing a detailed understanding of the relationship between interfacial ET processes, surface structure and charge, and mineral semiconducting properties. We focused on the Fe(III)-oxides and oxyhydroxides because of their geochemical preponderance, versatility in synthesis of compositionally, structurally, and morphologically tailored phases, and because they are amenable to a wide range of surface and bulk properties characterization. In particular, reductive transformation of phases such as hematite (α-Fe_2O_3) and goethite (α-FeOOH) in aqueous solution can serve as excellent model systems for studies of electron conduction processes, as well as provide valuable insights into effect of nanoscale conductive materials on contaminant fate at DOE sites.

More specifically, the goal of the Iowa component of this project was to use stable Fe isotope measurements to simultaneously measure isotope specific oxidation states and concentrations of Fe at the hematite-water and goethite-water interface. This work builds on our previous work where we used an innovative combination of ^{57}Fe Mössbauer spectroscopy and high precision isotope ratio measurements (MC-ICP-MS) to probe the dynamics of the reaction of aqueous Fe(II) with goethite. Mössbauer spectroscopy detects ^{57}Fe only among all other Fe isotopes and we have capitalized on this to spectroscopically demonstrate Fe(II)-Fe(III) electron transfer between sorbed Fe(II) and Fe(III) oxides (Handler, et al., 2009; Gorski, et al. 2010; Rosso et al., 2010). By combining the Mössbauer spectroscopy and stable isotopes measurements, we have been able to simultaneously track the oxidation state and isotope concentration of the bulk Fe oxide and aqueous Fe. One of our most compelling findings is that despite the apparent stability of the Fe(II)-goethite system, there is actually a tremendous amount of Fe atom cycling occurring between the aqueous phase and the bulk goethite as indicated by the isotopic composition of both phases approaching the mass balance average (Handler et al., 2009).

How such extensive re-crystallization and Fe atom exchange can occur with no significant morphological change is a fascinating question. Based on previous work from PI Rosso's group showing that a potential gradient across hematite crystal faces leads to conduction through hematite and growth and dissolution at separate crystal faces we proposed that a redox-driven recrystallization could be occurring that would explain the extensive mixing observed with the isotope data. From our previous studies utilizing Mössbauer spectroscopy, we know that sorption of Fe(II) onto goethite results in electron transfer between the sorbed Fe(II) and the structural Fe(III) in goethite. Oxidation of the sorbed Fe(II) produces growth of goethite on goethite (i.e., homoepitaxy), as well as injection of an electron into goethite. It is possible that electron transfer from sorbed Fe(II) occurs across a potential gradient, and that Fe(II) atoms are dissolved at a different location on the goethite surface. These newly-reduced Fe(II) atoms could then dissolve into the aqueous phase, exposing fresh Fe(III) goethite to the aqueous phase. Through a repeated series of these five steps of sorption–electron transfer–crystal growth–conduction–dissolution, a redox-driven conveyor belt, could be established that would allow all of the goethite to be

eventually exposed to the aqueous phase and exchanged. This surface-mediated recrystallization process would result in similar Fe isotope distributions in the aqueous phase and goethite particle, as we have observed here. It would also result in a stable aqueous Fe(II) concentration, if there were equal rates of goethite growth and dissolution.

Project Publications

1. Robert M. Handler, Andrew Frierdich, Clark M. Johnson, Kevin M. Rosso, Brian L. Beard, Chongmin Wang, Drew E. Latta, Anke Neumann, Timothy Pasakarnis, W.A.P.J. Premaratne, Michelle M. Scherer, Fe(II)-catalyzed recrystallization of goethite revisited. *Environ Sci Technol* **2014**, 48, 11302−11311. DOI: 10.1021/es503084u.
2. Frierdich, A.J., Helgeson, M., Liu C., Wang, C., Rosso K.M., Scherer M.M. Iron atom exchange between hematite and aqueous Fe(II). *Environ Sci Technol* **2015**, *14,* 8479-8486. DOI. 10.1021/acs.est.5b012.
3. Drew E. Latta, Piotr Zarzycki, Vitaly Alexandrov, Kevin M. Rosso, Michelle M. Scherer. Exploring the energetics of Fe(II)-Fe(III)$_{Goethite}$ electron transfer. **In Prep.**

Summary of Project Results

Fe Exchange between aqueous Fe(II) and goethite. Results from enriched ^{57}Fe isotope tracer experiments have shown that atom exchange can occur between structural Fe in Fe(III) oxides and aqueous Fe(II) with no formation of secondary minerals or change in particle size or shape. We derived a mass balance model to quantify the extent of Fe atom exchange between goethite and aqueous Fe(II) that accounts for different Fe pool sizes. We used this model to reinterpret our previous work and to quantify the influence of particle size and pH on extent of goethite exchange with aqueous Fe(II). Consistent with our previous interpretation, substantial exchange of goethite occurred at pH 7.5 (≈ 90%) and we observed little effect of particle size between nanogoethite (average size of 81 x 11 nm; ≈ 110 m^2/g) and microgoethite (average size of 590 x 42 nm; ≈ 40 m^2/g). Despite ≈ 90% of the bulk goethite exchanging at pH 7.5, we found no change in mineral phase, average particle size, crystallinity, or reactivity after reaction with aqueous Fe(II). At a lower pH of 5.0, no net sorption of Fe(II) was observed and significantly less exchange occurred accounting for less than the estimated proportion of surface Fe atoms in the particles. Particle size appears to influence the amount of exchange at pH 5.0 and we suggest that aggregation and surface area may play a role. Results from sequential chemical extractions indicate that ^{57}Fe accumulates in extracted Fe(III) goethite components. Isotopic compositions of the extracts indicate that a gradient of ^{57}Fe develops within the goethite with more accumulation of ^{57}Fe occurring in the more easily extracted Fe(III) that may be nearer to the surface. **This work was published in *Environmental Science & Technology* in 2014 (Handler, 2014).**

Fe Exchange between aqueous Fe(II) and hematite. Aqueous Fe(II) has been shown to exchange with structural Fe(III) in goethite, magnetite, and ferrihydrite. It remains unclear, however, whether aqueous Fe(II) undergoes similar exchange reactions with hematite, a ubiquitous Fe(III) oxide mineral. Analogous experiments with Fe(II)/hematite have never previously been performed and we performed a series of experiments to evaluate Fe(II)-catalyzed recrystallization of hematite.

To evaluate the extent of exchange between hematite and aqueous Fe(II), we reacted hematite of two different particle sizes with a 1 mM ^{57}Fe-enriched aqueous Fe(II) solution buffered at pH 7.0 and tracked the concentration and isotopic composition of Fe(II)$_{aq}$, HCl extracted Fe(II) (Fe(II)$_{extr}$), and hematite over time. After initiating the experiment, the concentration of Fe(II)$_{aq}$ decreases and reaches a steady-state value within 1 day (SI Figure S1). The Fe(II)$_{aq}$ concentration remains constant (within error)

for the remainder of the experiment (SI Table S1). The $Fe(II)_{aq}$ lost from solution is ~equal to the 0.4 M HCl extractable Fe(II) component (SI Table S1), thus closing the Fe(II) mass balance within error. Despite quantitative recovery of Fe(II), and a sorption-desorption steady-state, the iron isotope composition of all three iron components (i.e., $Fe(II)_{aq}$, $Fe(II)_{extr}$, hematite) change throughout the reaction revealing dynamics not apparent from the iron concentration measurements (**Figure 1**).

Since the aqueous Fe(II) was heavily enriched for ^{57}Fe, the initial iron isotope composition of $Fe(II)_{aq}$ is almost entirely ^{57}Fe ($f^{57}Fe$=0.92±0.02). The fraction of ^{57}Fe in $Fe(II)_{aq}$ immediately begins to decrease after adding hematite, whereas the amounts of ^{56}Fe and ^{54}Fe in the aqueous phase increase (**Figure 1**). Loss of Fe(II) from solution via net sorption to hematite (or, any unidirectional process) is not responsible for the changing isotopic composition in solution since natural mass-dependent isotope fractionation of iron is insignificant on the scale of our enriched isotope study. For example, kinetic and equilibrium iron isotope fractionations are on the order of a few per mil and would thus only alter $f^{57}Fe$ values by less than 0.0001. Consequently, the observed decrease in $f^{57}Fe$ and increase in $f^{56}Fe$ and $f^{54}Fe$ of $Fe(II)_{aq}$ indicates that the $Fe(II)_{aq}$ is exchanging with structural Fe(III) in hematite.

The HCl extractable Fe(II) and hematite also exhibit substantial changes in their isotopic composition, with $f^{57}Fe$ in hematite increasing (**Figure 2**) and $f^{56}Fe$ decreasing (SI Table S1) as expected if exchange was occurring. Similarly, the fraction of ^{54}Fe of hematite underwent a measureable, but substantially smaller, change during reaction between $Fe(II)_{aq}$ and hematite (SI Table S1). The changes in the iron isotope composition of hematite is consistent with incorporation of the original ^{57}Fe-enriched Fe(II) from solution. The iron isotope composition of $Fe(II)_{extr}$ is identical (within error) to $Fe(II)_{aq}$ for nearly every time point (**Figure 2**). Similar iron isotope compositions of these components demonstrates that they are in isotopic equilibrium and thus $f^{n}Fe$ values of $Fe(II)_{aq}$ can be directly substituted into eq 2 for $f^{t}_{Fe(II)}$ to yield accurate calculations of the percent of iron exchange in hematite.

Calculations of percent iron exchange in hematite, via $f^{57}Fe$ of $Fe(II)_{aq}$, shows that substantially different amounts of exchange occur for 27 m^2 g^{-1} hematite and 54 m^2 g^{-1} hematite, with the 54 m^2 g^{-1} hematite exchanging nearly 5 times as much of its structural Fe(III) as the 27 m^2 g^{-1} hematite (**Figure 3**). The extent of exchange observed for 27 m^2 g^{-1} hematite (i.e., ~4%) is almost exactly one surface iron layer (See SI for calculation of the percentage of surface iron atoms), suggesting that little to no exchange has occurred for the bulk iron atoms in the mineral. However, almost 3 times the amount of surface iron atoms in 54 m^2 g^{-1} hematite have exchanged with $Fe(II)_{aq}$, demonstrating that the bulk iron in these particles is accessible to exchange under these conditions (pH 7.0 and 1 mM aqueous Fe(II)).

The significant effect of particle size on extent of exchange may explain why there is some discrepancy in the literature with several studies indirectly suggesting Fe(II) exchanges with hematite [13-16, 21, 23, 24, 26], and others, some including direct isotope measurements,[11] indicating that exchange does not occur.[11, 17] Jeon et al. (2003), for example, reacted $Fe(II)_{aq}$ with hematite in the presence of sorbed divalent metals (e.g., Ni(II)) and reported no effect on metal fixation[17], while in some of our previous work we observe both the incorporation of Ni into pure hematite[16] and the release of Ni from substituted hematite when $Fe(II)_{aq}$ was present.[15] Iron atom exchange has also been proposed as the mechanism for iron isotope fractionation between $Fe(II)_{aq}$ and hematite during abiotic reactions of the two components and during microbial iron reduction experiments. In these experiments, however, only roughly one surface iron layer was thought to participate in exchange.[23, 24, 26] Pedersen et al. (2005) directly measured isotopic exchange between $Fe(II)_{aq}$ and ^{55}Fe-labeled hematite and found that no ^{55}Fe was found in the $Fe(II)_{aq}$ component after ~25 days, and thus concluded that $Fe(II)_{aq}$ does not exchange with hematite.[11] Pedersen et al. (2005), however, used hematite particles with a surface area of 19 m^2 g^{-1} which are presumably larger than the 27 and 54 m^2 g^{-1} particles used in this study and based on our results would be expected to have

limited exchange. Indeed, in many of the hematite studies, the hematite particles were relatively large (e.g., up to micron-sized) and low specific surface area (e.g., ~10 $m^2 g^{-1}$).[17, 23, 24, 26] Limited exchange for low surface area hematite particles is consistent with the low amount of iron exchange we observed here for 27 $m^2 g^{-1}$ hematite (~1 surface iron layer) suggesting that prior conclusions of one iron octahedral surface iron layer participating in exchange are reasonable.[26]

Effect of Fe(II) Sorption on Extent of Hematite Exchange. While it is clear that particle size influences the extent of exchange for hematite, previous work with goethite suggests that pH and the amount of sorbed Fe(II) may also be important variables to consider. In our prior work, we have shown that sorbed Fe(II) is proportional to the amount of iron atom exchange in goethite when the solution pH is varied.[9, 27] Here, we modify the amount of sorbed Fe(II) on hematite by conducting experiments with variable initial $Fe(II)_{aq}$ concentrations and by changing the solution pH to test how these parameters affect the amount of iron exchange in hematite. First, hematite was reacted with a fixed Fe(II) concentration (i.e., $[Fe(II)_{aq}]_0$~1 mM) in solutions of variable pH (5.5-8.0). Second, the initial aqueous Fe(II) concentration was varied (0.5-4.0 mM) with solution pH fixed at 7.5 (**Table 1**).

As solution pH is increased from 5.5 to 7.5, the amount of atom exchange between $Fe(II)_{aq}$ and 54 $m^2 g^{-1}$ hematite increases from ~10% to 40% (**Table 1**, **Figure 4**). Note that the Pedersen et al. (2005) study was done at pH 6.5 and the combination of both larger particles and low pH most likely explain why no exchange was observed. As expected, as pH increases, the amount of sorbed Fe(II) also increases which is typical for cation sorption on oxide surfaces (**Figure 4B**). However, at the highest pH value tested (pH 8.0), while the amount of Fe(II) continued to increase, the amount of exchange in hematite was found to be less (**Figure 4B**). Interestingly, the lesser amount of iron exchange at pH 8.0 occurs as the sorbed Fe(II) exceeds the theoretical surface site capacity of hematite of 224 mmole g^{-1}, based on a density of 2.5 sites nm^{-2}.[17, 30] To determine if the relationship between iron exchange and pH is controlled simply by the amount of sorbed Fe(II), as modified by pH, we conducted a second set of experiments at pH 7.5 (apparent optimal exchange) and varied the $Fe(II)_{aq}$ concentration to induce variable amounts of Fe(II) sorption.

The effect of initial $Fe(II)_{aq}$ concentrations on the extent of iron exchange in hematite initially reveals a somewhat counterintuitive result, with the amount of exchange progressively decreasing as the amount of Fe(II) in solution increases (**Table 1**, **Figure 5**). As the concentration of Fe(II) increases to 4 mM, the amount of atom exchange in hematite decreases to amounts approaching a single iron surface layer (i.e., ~9% for 54 $m^2 g^{-1}$ hematite). On the other hand, at the lower end of initial $Fe(II)_{aq}$ concentrations (0.5 mM) we see over 40% exchange in hematite. The uptake behavior of Fe(II) shows that Fe(II) sorption is not proportional to $Fe(II)_{aq}$ added but rather approaches a maximum value consistent with surface site saturation behavior typical for sorption reactions (**Figure 5B**). Indeed, Fe(II) sorption is modeled well using a Langmuir isotherm (SI Figure S2). Within error, added $Fe(II)_{aq}$ concentrations from 1 to 4 mM are potentially saturating the surface sites with sorbed Fe(II) and, as we observed for the variable pH experiment, this leads to a decrease in the amount of iron exchange (SI Figure S3).

The observation that high concentrations of $Fe(II)_{aq}$ begin to inhibit and decrease the extent of exchange in hematite is, at first, counterintuitive if $Fe(II)_{aq}$ is viewed as a catalyst for activating Fe(III) oxide recrystallization. However, if one considers the possibility of altering the surface potentials of hematite (e.g., as discussed in Yanina and Rosso (2008)), or forming a discrete Fe(II)-bearing surface layer (e.g., as reported in Larese-Casanova et al. (2007)), one may conceptualize that electron transfer between Fe(II) and hematite becomes less energetically favorable as Fe(II) accumulates on the hematite surface. Surface potential differences on crystallographically distinct surfaces of hematite, for example, have been shown to result in bulk electron conduction through the mineral in the presence of $Fe(II)_{aq}$[21].

Surface modification, via Fe(II) or oxalate sorption, substantially changes this potential difference and thus the favorability for Fe(II)-Fe(III) electron transfer, and presumably atom exchange[21]. Similarly, the inhibition of $Fe(II)_{aq}$ exchange with hematite that we observe at monolayer surface coverage of Fe(II) may result from changes in the surface potentials on hematite and hence decrease the energetics of electron transfer to and conduction through the solid to prevent further exchange. Although Fe(II) oxidation by the underlying Fe(III) in hematite has been demonstrated by ^{57}Fe Mossbauer spectroscopy,[3, 13] Larese-Casanova et al. (2007) clearly showed electron transfer was favorable only until monolayer coverage of hematite by Fe(II). Upon surface-site saturation, a stable, sorbed Fe(II) species was observed, indicating that Fe(II)-Fe(III) electron transfer no longer occurred. Importantly, all of the original Fe(II) added was oxidized by Fe(III) in hematite below monolayer coverage. Thus, the decrease in atom exchange between $Fe(II)_{aq}$ and hematite observed at monolayer coverage of the hematite surface is consistent with the inhibition of electron transfer observed by Larese-Casanova et al. (2007).

Similar Fe(II) passivation has been described in the geomicrobiology literature. For example, it has been shown that sorbed Fe(II) on crystalline Fe(III) oxide surfaces (e.g., goethite, hematite) limits the amount of Fe(III) reduction during anaerobic microbial respiration,[31, 32] with a prospective mechanism involving the formation of an Fe(II)-bearing layer[33] or alteration of the surface potential.[34] It is recognized that Fe(II) surface complexes on Fe(III) oxides exhibit different redox potentials than $Fe(II)_{aq}$[2, 35], thus rendering $Fe(II)_{sorb}$ more reactive towards the reduction of contaminants than $Fe(II)_{aq}$[36-40]. Furthermore, Fe(II) is known to increase the reactivity of zero-valent iron (Fe^0)[41] and even depassivate Fe^0 that has accumulated Fe(III) oxide coatings.[42] Even though sorbed Fe(II) may increase the surface reactivity of Fe(III) oxides in terms of electron transfer to aqueous/sorbed species, its effect on overall surface potential and ability to affect electron transfer to and conduction within the mineral remains unclear. In a recent classical molecular dynamics simulation study of the adsorption and interfacial electron exchange of Fe(II) on perfect hematite (001) surfaces showed that while stable adsorbed surface complexes could be found, the electron exchange process is generally unfavorable (Kerisit et al., 2015, JPCC, in revision). A similar conclusion was found for Fe(II) interaction with perfect low-index goethite surfaces using the same classical force field and methods[43] as well as separately using quantum mechanical methods (Alexandrov and Rosso 2015, PCCP, in review). However, in this latter study it was also found that surface defects such as oxygen vacancies increased the driving force for the interfacial electron transfer from adsorbed Fe(II) to lattice Fe(III) via a local charge imbalance that is alleviated by injection of the electron. It is thus conceivable that in the present experiments, at low surface coverage of sorbed Fe(II), the main interaction with the hematite solid is interfacial electron transfer driven by concomitant healing of surface structure imperfections through Fe(III) addition and oxygen ligand exchange, which reconstructs surfaces to low energy stoichiometric and charge neutral configurations. At increasing surface coverage, sorbed Fe(II) thereby interacts with increasingly structurally ordered hematite surfaces, and thus the propensity for interfacial electron transfer and atom exchange diminishes.

Though the exact mechanism remains speculative, the inhibitive effect of increasing Fe(II) on iron-atom exchange between $Fe(II)_{aq}$ and hematite is evident, suggesting that, perhaps counter-intuitively, low concentrations of $Fe(II)_{aq}$ well below surface saturation will have the greatest effect on the Fe(II)-Fe(III) interfacial electron and atom exchange between $Fe(II)_{aq}$ and Fe(III) oxide minerals.

Particle characterization before and after reaction with $Fe(II)_{aq}$. Prior ex situ characterization work has shown that goethite does not undergo significant changes in particle size, shape, crystallinity, or bulk reactivity even after extensive (~90%) iron-atom exchange with $Fe(II)_{aq}$.[8, 9] Although we observe less exchange for hematite, as compared to goethite, a substantial amount of exchange does occur, including more extensively than just the outermost surface iron atoms, and thus subtle changes in the chemical or physical properties of hematite may assist with elucidating the exchange mechanism. Hematite solids

were thus collected following reaction in a pH 7.5 buffered fluid in the absence and presence of 1 mM Fe(II) for 32 days and analyzed by XRD, high-resolution transmission electron microscopy (HR-TEM), and proton-promoted and reductive dissolution.

XRD shows that both 27 and 54 $m^2 g^{-1}$ hematite collected after reaction with Fe(II) contain no other crystalline impurities (SI Figure S4). Hence, the iron exchange that we observe (e.g., **Figure 3**) does not involve a mineralogical transformation. Although both materials are mineralogically pure at the resolution of XRD, clear differences in the line widths of 27 and 54 $m^2 g^{-1}$ hematite are present (SI Figure 4B). Broader XRD peaks for 54 $m^2 g^{-1}$ hematite reveal a smaller coherent scattering domain size (i.e., smaller crystallites) for this material. Differences in peak intensities are another useful tool for exploring the stoichiometry of hematite as the (104) reflection relates to iron occupancy whereas (113) depends solely on the oxygen lattice. [44-46] Consequently, the relative amount of hydration (i.e., structural H^+ which is charge balanced by iron vacancies), which is typical for low temperature aqueous syntheses,[28] may be assessed. The smaller (104):(113) ratio for 54 $m^2 g^{-1}$ hematite suggests a greater degree of hydration relative to 27 $m^2 g^{-1}$ hematite. Changes in the XRD peak intensities and widths of 54 $m^2 g^{-1}$ hematite are apparent when this material is reacted with Fe(II) (SI Figure S4), as compared to the hematite suspended in an Fe(II)-free control, suggesting a higher degree of crystallinity and a lesser amount of hydration.

The kinetics of reductive dissolution of 27 and 54 $m^2 g^{-1}$ hematite by ascorbic acid appear to be proportional to mineral surface area, with 54 $m^2 g^{-1}$ hematite undergoing nearly twice as much dissolution (**Figure 6**). The rate and extent of dissolution of 27 $m^2 g^{-1}$ hematite is identical (within error) for both the control and the Fe(II)-reacted sample. However, significant differences are observed for 54 $m^2 g^{-1}$, with less overall dissolution occurring for the sample that was reacted with $Fe(II)_{aq}$. Furthermore, the divergence of the reacted and unreacted 54 $m^2 g^{-1}$ hematite does not occur until ~6-8% total dissolution (**Figure 6**), which is close to the percentage of surface iron atoms. Similar results are observed when hematite undergoes proton-promoted dissolution in HCl (SI Figure S5), although the conclusions are less certain due to a greater degree of error in the data. The differences in reductive dissolution observed here may be related to the degree of hydration of hematite following reaction with $Fe(II)_{aq}$.

Jang et al., 2007 suggested that the hydration extent of hematite increases the minerals solubility.[47] Since 54 $m^2 g^{-1}$ is less hydrated following reaction with Fe(II), this may explain its lesser reactivity in terms of its susceptibility to reductive dissolution. The finding that 54 $m^2 g^{-1}$ hematite is less reactive following reaction with Fe(II) is in contrast to the observations of Handler et al. (2014) who found that no change in the reactivity of goethite occurred after near-complete (~90%) iron atom exchange with $Fe(II)_{aq}$. In the case of goethite, however, less than one surface iron layer was reductively dissolved and thus may not have sufficiently probed the "bulk" goethite reactivity.

Ex situ HR-TEM imaging of the hematite nanoparticles before and after reaction were consistent with the XRD analyses, showing that no new phases emerge upon reaction with aqueous Fe(II) (SI Figure S6). Qualitative visual comparison of the particle sizes, shapes, and crystallinity of particle ensembles and isolated single particles showed no obvious differences resulting from reaction. As is the case microscopically documented for goethites,[8, 9] the particles appear unmodified in terms of these characteristics despite the significant Fe(II)-catalyzed atom exchange that occurs.

This work was published in *Environmental Science & Technology* in 2015 (Frierdich, 2015).

REFERENCES

1. Williams, A. G. B.; Scherer, M. M., Spectroscopic evidence for Fe(II)-Fe(III) electron transfer at the iron oxide-water interface. *Environ. Sci. Technol.* **2004,** *38*, 4782–4790.

2. Silvester, E.; Charlet, L.; Tournassat, C.; Gehin, A.; Greneche, J.-M.; Liger, E., Redox potential measurements and Mössbauer spectrometry of FeII adsorbed onto FeIII (oxyhydr)oxides. *Geochim. Cosmochim. Acta* **2005,** *69*, (20), 4801-4815.

3. Larese-Casanova, P.; Scherer, M. M., Fe(II) sorption on hematite: New insights based on spectroscopic measurements. *Environ. Sci. Technol.* **2007,** *41*, 471–477.

4. Cwiertny, D. M.; Handler, R. M.; Schaefer, M. V.; Grassian, V. H.; Scherer, M. M., Interpreting nanoscale size-effects in aggregated Fe-oxide suspensions: Reaction of Fe(II) with Goethite. *Geochim. Cosmochim. Acta* **2008,** *72*, 1365–1380.

5. Frierdich, A. J.; Beard, B. L.; Reddy, T. R.; Scherer, M. M.; Johnson, C. M., Iron isotope fractionation between aqueous Fe(II) and goethite revisited: New insights based on a multi-direction approach to equilibrium and isotopic exchange rate modification. *Geochim. Cosmochim. Acta* **2014,** *139*, 383-398.

6. Frierdich, A. J.; Beard, B. L.; Scherer, M. M.; Johnson, C. M., Determination of the $Fe(II)_{aq}$-magnetite equilibrium iron isotope fractionation factor using the three-isotope method and a multi-direction approach to equilibrium *Earth Planet. Sc. Lett.* **2014,** *391*, 77-86.

7. Gorski, C. A.; Handler, R. M.; Beard, B. L.; Pasakarnis, T.; Johnson, C. M.; Scherer, M. M., Fe Atom Exchange between Aqueous Fe2+ and Magnetite. *Environ. Sci. Technol.* **2012,** *46*, 12399–12407.

8. Handler, R. M.; Beard, B. L.; Johnson, C. M.; Scherer, M. M., Atom exchange between aqueous Fe(II) and goethite: An Fe isotope tracer study. *Environ. Sci. Technol.* **2009,** *43*, 1102–1107.

9. Handler, R. M.; Frierdich, A. J.; Johnson, C. M.; Rosso, K. M.; Beard, B. L.; Wang, C.; Latta, D. E.; Neumann, A.; Pasakarnis, T.; Premaratne, W. A. P. J.; Scherer, M. M., Fe(II)-catalyzed recrystallization of goethite revisited. *Environ. Sci. Technol.* **2014,** *48*, 11302–11311.

10. Latta, D. E.; Bachman, J. E.; Scherer, M. M., Fe electron transfer and atom exchange in goethite: Influence of Al-substitution and anion sorption. *Environ. Sci. Technol.* **2012,** *46*, 10614–10623.

11. Pedersen, H. D.; Postma, D.; Jakobsen, R.; Larsen, O., Fast transformation of iron oxyhydroxides by the catalytic action of aqueous Fe(II). *Geochim. Cosmochim. Acta* **2005,** *69*, 3967–3977.

12. Wu, L.; Beard, B. L.; Roden, E. E.; Johnson, C. M., Stable iron isotope fractionation between aqueous Fe(II) and hydrous ferric oxide. *Environ. Sci. Technol.* **2011,** *45*, 1847–1852.

13. Rosso, K. M.; Yanina, S. V.; Gorski, C. A.; Larese-Casanova, P.; Scherer, M. M., Connecting observations of hematite (α-Fe_2O_3) growth catalyzed by Fe(II). *Environ. Sci. Technol.* **2010,** *44*, 61–67.

14. Frierdich, A. J.; Catalano, J. G., Controls on Fe(II)-activated trace element release from goethite and hematite. *Environ. Sci. Technol.* **2012,** *46*, 1519–1526.

15. Frierdich, A. J.; Catalano, J. G., Fe(II)-mediated reduction and repartitioning of structurally incorporated Cu, Co, and Mn in iron oxides. *Environ. Sci. Technol.* **2012,** *46*, 11070–11077.

16. Frierdich, A. J.; Luo, Y.; Catalano, J. G., Trace element cycling through iron oxide minerals during redox-driven dynamic recrystallization. *Geology* **2011,** *39*, 1083–1086.

17. Jeon, B.-H.; Dempsey, B. A.; Burgos, W. D.; Royer, R. A., Sorption kinetics of Fe(II), Zn(II), Co(II), Ni(II), Cd(II), and Fe(II)/Me(II) onto hematite. *Water Res.* **2003,** *37*, 4135–4142.

18. Cooper, C. D.; Neal, A. L.; Kukkadapu, R. K.; Brewe, D.; Coby, A.; Picardal, F. W., Effects of sediment iron mineral composition on microbially mediated changes in divalent metal speciation: Importance of ferrihydrite. *Geochim. Cosmochim. Acta* **2005,** *69*, 1739–1754.

19. Cooper, C. D.; Picardal, F.; Rivera, J.; Talbot, C., Zinc immobilization and magnetite formation via ferric oxide reduction by *Shewanella* putrefaciens 200. *Environ. Sci. Technol.* **2000,** *34*, 100-106.

20. Coughlin, B. R.; Stone, A. T., Nonreversible adsorption of divalent metal ions (Mn(II), Co(II), Ni(II), Cu(II), and Pb(II)) onto goethite: Effects of acidification, Fe(II) addition, and picolinic acid addition. *Environ. Sci. Technol.* **1995,** *29*, 2445–2455.

21. Yanina, S. V.; Rosso, K. M., Linked reactivity at mineral-water interfaces through bulk crystal conduction. *Science* **2008,** *320*, 218–222.

22. Catalano, J. G.; Fenter, P.; Park, C.; Zhang, Z.; Rosso, K. M., Structure and oxidation state of hematite surfaces reacted with aqueous Fe(II) at acidic and neutral pH. *Geochim. Cosmochim. Acta* **2010,** *74*, 1498–1512.

23. Crosby, H. A.; Johnson, C. M.; Roden, E. E.; Beard, B. L., Coupled Fe(II)-Fe(III) electron and atom exchange as a mechanism for Fe isotope fractionation during dissimilatory iron oxide reduction. *Environ. Sci. Technol.* **2005,** *39*, 6698–6704.

24. Crosby, H. A.; Roden, E. E.; Johnson, C. M.; Beard, B. L., The mechanisms of iron isotope fractionation produced during dissimilatory Fe(III) reduction by *Shewanella putrefaciens* and *Geobacter sulfurreducens*. *Geobiology* **2007,** *5*, 169–189.

25. Wu, L.; Beard, B. L.; Roden, E. E.; Johnson, C. M., Influence of pH and dissolved Si on Fe isotope fractionation during dissimilatory microbial reduction of hematite. *Geochim. Cosmochim. Acta* **2009,** *73*, 5584-5599.

26. Wu, L.; Beard, B. L.; Roden, E. E.; Kennedy, C. B.; Johnson, C. M., Stable Fe isotope fractionations produced by aqueous Fe(II)-hematite surface interactions. *Geochim. Cosmochim. Acta* **2010,** *74*, 4249–4265.

27. Reddy, T. R.; Frierdich, A. J.; Beard, B. L.; Johnson, C. M., The effect of pH on stable iron isotope exchange and fractionation between aqueous Fe(II) and goethite. *Chem. Geol.* **2015**, doi:10.1016/j.chemgeo.2015.01.018.

28. Schwertmann, U.; Cornell, R. M., *Iron oxides in the laboratory: Preparation and characterization*. 2nd ed.; Wiley-VCH: Weinheim, 2000; p 188.

29. Stookey, L. L., Ferrozine-a new spectrophotometric reagent for iron. *Anal. Chem.* **1970,** *42*, 779-781.

30. Jeon, B.-H.; Dempsey, B. A.; Burgos, W. D.; Royer, R. A., Reactions of ferrous iron with hematite. *Colloids Surf. A* **2001,** *191*, 41-55.

31. Roden, E. E.; Zachara, J. M., Microbial reduction of crystalline iron(III) oxides: Influence of oxide surface area and potential for cell growth. *Environ. Sci. Technol.* **1996,** *30*, (5), 1618-1628.

32. Urrutia, M. M.; Roden, E. E.; Zachara, J. M., Influence of aqueous and solid-phase Fe(II) complexants on microbial reduction of crystalline iron(III) oxides. *Environ. Sci. Technol.* **1999,** *33*, (22), 4022-4028.

33. Hansel, C. M.; Benner, S. G.; Nico, P.; Fendorf, S., Structural constraints of ferric (hydr)oxides on dissimilatory iron reduction and the fate of Fe(II). *Geochim. Cosmochim. Acta* **2004,** *68*, (15), 3217-3229.

34. Roden, E. E.; Urrutia, M. M., Influence of biogenic Fe(II) on bacterial crystalline Fe(III) oxide reduction. *Geomicrobiol. J.* **2002,** *19*, (2), 209-251.

35. Orsetti, S.; Laskov, C.; Haderlein, S. B., Electron transfer between iron minerals and quinones: Estimating the reduction potential of the Fe(II)-goethite surface from AQDS speciation. *Environ. Sci. Technol.* **2013,** *47*, (24), 14161-14168.

36. Buerge, I. J.; Hug, S., J., Influence of mineral surfaces on chromium(VI) reduction by iron(II). *Environ. Sci. Technol.* **1999,** *33*, 4285–4291.

37. Elsner, M.; Schwarzenbach, R. P.; Haderlein, S., Reactivity of Fe(II)-bearing minerals toward reductive transformation of organic contaminants. *Environ. Sci. Technol.* **2004,** *38*, 799–807.

38. Felmy, A. R.; Moore, D. A.; Rosso, K. M.; Qafoku, O.; Rai, D.; Buck, E. C.; Ilton, E. S., Heterogeneous Reduction of PuO_2 with Fe(II): Importance of the Fe(III) Reaction Product. *Environ. Sci. Technol.* **2011,** *45*, 3952–3958.

39. Liger, E.; Charlet, L.; Cappellen, P. V., Surface catalysis of uranium(VI) reduction by iron(II). *Geochim. Cosmochim. Acta* **1999,** *63*, 2939–2955.

40. Strathmann, T. J.; Stone, A. T., Mineral surface catalysis of reactions between Fe^{II} and oxime carbamate pesticides. *Geochim. Cosmochim. Acta* **2003,** *67*, 2775–2791.

41. Huang, Y. H.; Zhang, T. C., Effects of dissolved oxygen on formation of corrosion products and concomitant oxygen and nitrate reduction in zero-valent iron systems with or without aqueous Fe^{2+}. *Water Res.* **2005,** *39*, (9), 1751-1760.

42. Liu, T.; Li, X.; Waite, T. D., Depassivation of aged Fe^0 by ferrous ions: Implications to contaminant degradation. *Environ. Sci. Technol.* **2013,** *47*, (23), 13712-13720.

43. Zarzycki, P.; Kerisit, S.; Rosso, K. M., Molecular dynamics study of Fe(II) adsorption, electron exchange, and mobility at goethite (α-FeOOH) surfaces. *J. Phys. Chem. C* **2015,** *119*, (6), 3111-3123.

44. Wolska, E., The structure of hydrohematite. *Zeitschrift fur Kristallographie* **1981,** *154*, 69-75.

45. Wolska, E., Relations between the existence of hydroxyl ions in the anionic sublattice of hematite and its infrared and X-ray characteristics. *Solid State Ionics* **1988,** *28-30, Part 2*, 1349-1351.

46. Wolska, E.; Szajda, W., Structural and spectroscopic characteristics of synthetic hydrohaematite. *J. Mater. Sci.* **1985,** *20*, (12), 4407-4412.

47. Jang, J.-H.; Dempsey, B. A.; Burgos, W. D., Solubility of Hematite Revisited: Effects of Hydration. *Environ. Sci. Technol.* **2007,** *41*, (21), 7303-7308.

TABLES

Table 1. Summary data for Fe(II) sorption and percent exchange of iron in hematite for reactions at variable pH and initial amounts of aqueous Fe(II).

pH	$[Fe(II)_{aq}]_0$ (mM)	Sorbed Fe(II) [b] (μmole g^{-1})	Hem Fe Ex [c] (%)
Variable pH			
5.5	0.97 (±0.02)[a]	23 (±26)	8.5 (±0.1)
6.5	0.97 (±0.02)	70 (±34)	25.0 (±2.0)
7.0	1.04 (±0.01)	163 (±24)	29.0 (±0.5)
7.5	0.97 (±0.02)	241 (±41)	38.0 (±8.0)
8.0	0.97 (±0.02)	323 (±13)	32.0 (±0.3)
Variable $Fe(II)_{aq}$			
7.5	0.52 (±0.04)	168 (±23)	41.0 (±3.0)
7.5	0.97 (±0.02)	241 (±41)	33.0 (±1.0)
7.5	2.00 (±0.00)	226 (±16)	21.0 (±2.0)
7.5	4.10 (±0.10)	288 (±99)	12.1 (±0.3)

[a] Error is the standard deviation (1σ) of replicate samples. [b] Calculated from the average of the last three $Fe(II)_{aq}$ concentration time points minus the initial $Fe(II)_{aq}$ concentration (see SI Tables S1-S3). [c] Taken as the last time point for each reaction (see Figures 4 and 5).

FIGURES

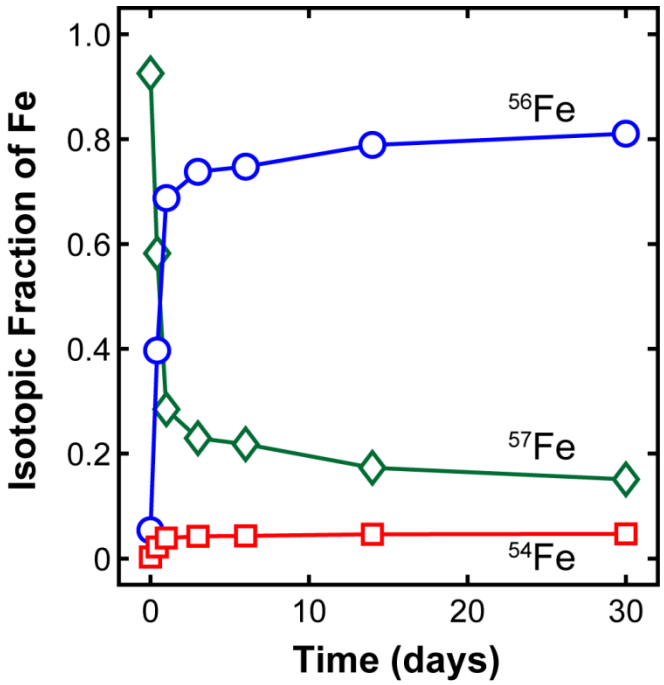

Figure 1. Temporal evolution of the iron-isotope fractions (eq 1) of $Fe(II)_{aq}$ during its reaction with hematite (50 nm, 54 m^2g^{-1}) at pH 7. Aqueous Fe(II) was initially enriched in ^{57}Fe (0.92), and hence depleted in ^{56}Fe (0.06) and ^{54}Fe (0.03). Hematite has a natural abundance iron-isotope composition (0.02, 0.92, and 0.05 for ^{57}Fe, ^{56}Fe, and ^{54}Fe, respectively) Conditions: $[Fe(II)_{aq}]_0$=1 mM, [Hem] = 2 g/L, 25 mM HEPES/KBr.

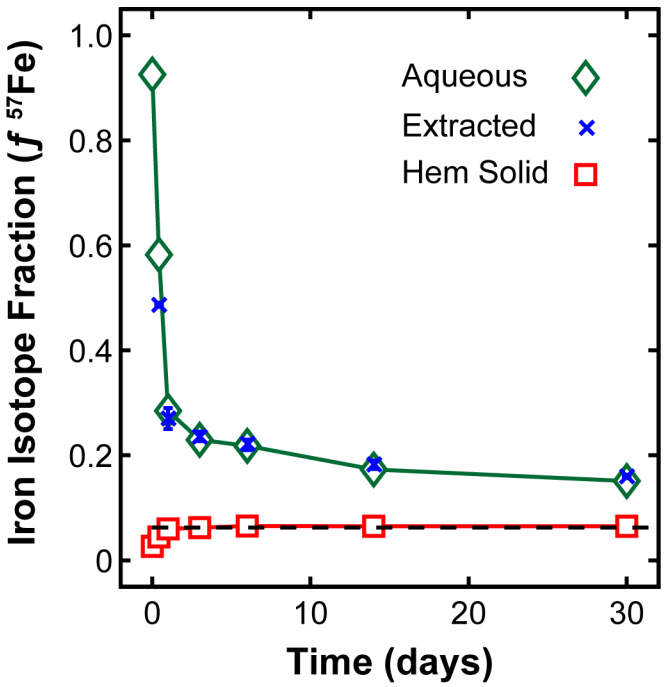

Figure 2. The fraction of ^{57}Fe in aqueous Fe(II), extracted Fe(II), and hematite over time. The horizontal dashed line is the calculated ^{57}Fe mass balance, and at complete exchange the f^{57}Fe for all components should approach this value. Conditions: $[Fe(II)_{aq}]_0$=1 mM, [Hem] = 2 g/L, 25 mM HEPES/KBr at pH 7.0.

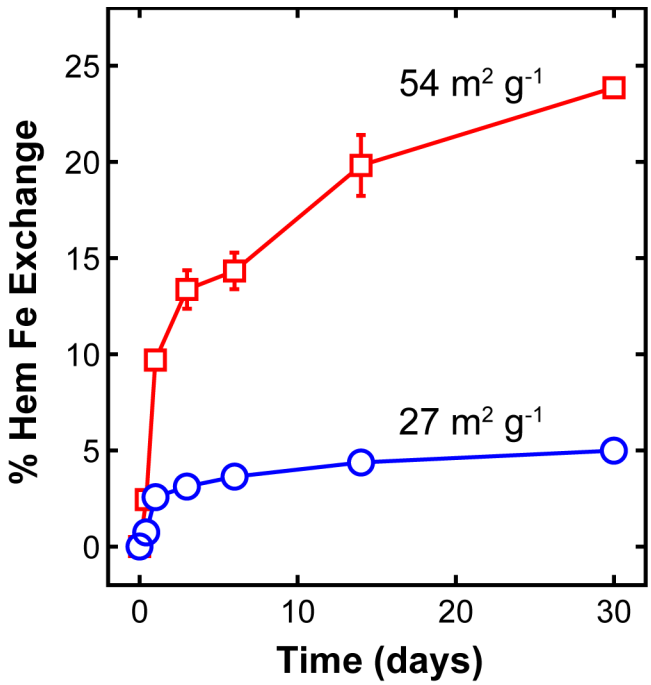

Figure 3. Percent exchange of Fe in hematite, as calculated from f^{57}Fe of Fe(II)aq (eq 2), over time for hematite of two particle sizes and specific surface areas. Conditions: $[Fe(II)_{aq}]_0$=1 mM, [Hem] = 2 g/L, 25 mM HEPES (pH 7)/KBr.

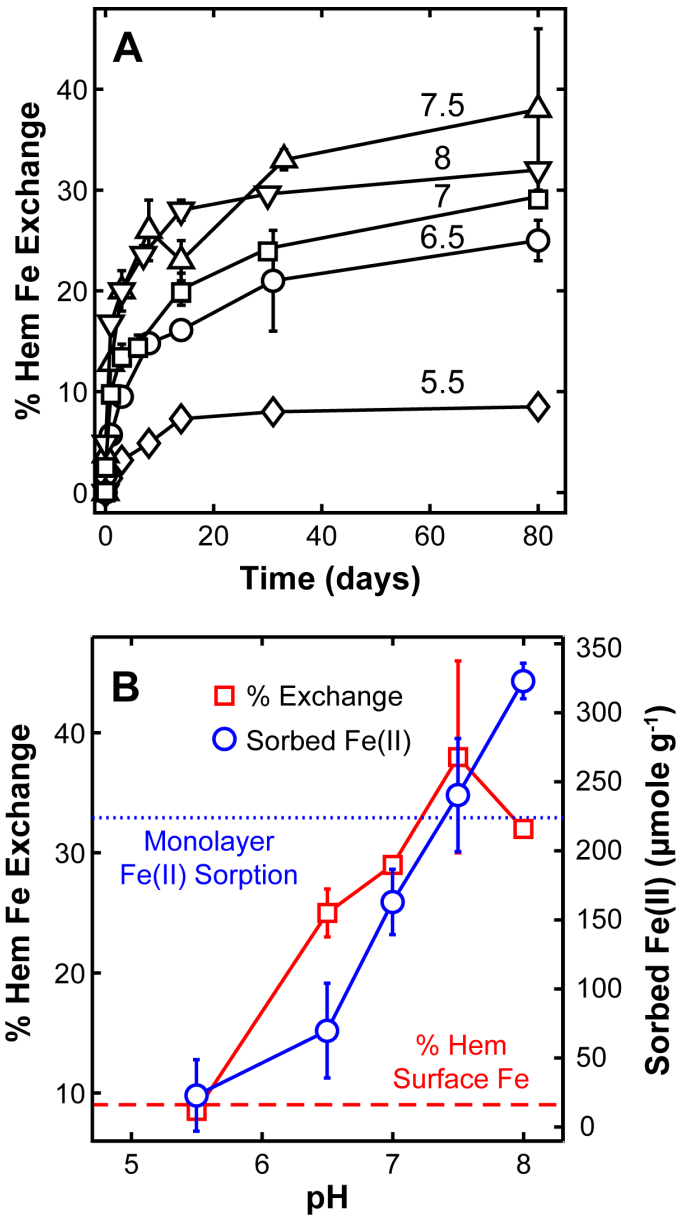

Figure 4. (A) Percent iron exchange over time for 54 m^2g^{-1} hematite with varying solution pH. **(B)** Effect of pH on percent iron exchange and corresponding Fe(II) sorption. Sorbed Fe(II) was calculated by taking the average of the last three time points for each reaction (SI Table S2,S3) and subtracting that value from the initial $Fe(II)_{aq}$ concentration (i.e., at time t=0). Exchange values takes as the last time point. Horizontal dotted line is the theoretical monolayer sorption capacity of hematite based on a surface site density of 2.5 sites nm^{-2}.[17] Dashed line is the percentage of iron atoms located at the surface (See SI for calculation). All reactions contained 2 g Hem L^{-1} with an initial $Fe(II)_{aq}$ concentration of 1 mM.

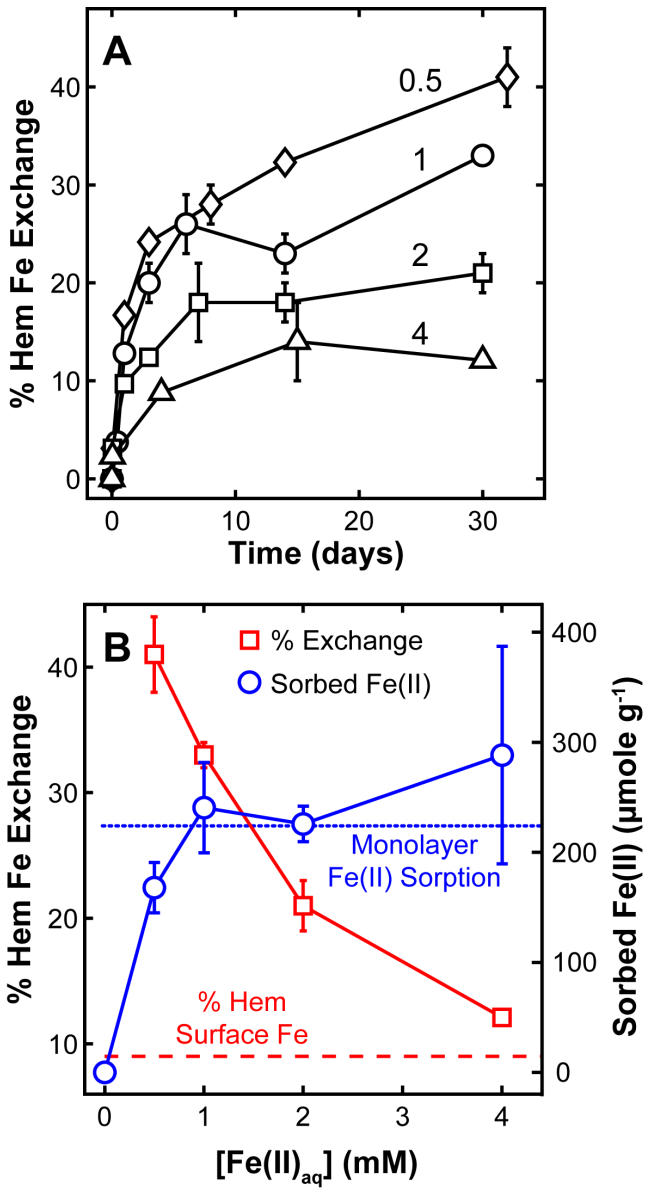

Figure 5. (A) Percent iron exchange over time for 54 $m^2 g^{-1}$ hematite at varying initial concentrations of aqueous Fe(II). **(B)** Effect of $Fe(II)_{aq}$ on percent iron exchange and corresponding Fe(II) sorption. Sorbed Fe(II) was calculated by taking the average of the last three time points for each reaction (SI Table S2,S3) and subtracting that value from the initial $Fe(II)_{aq}$ concentration (i.e., at time t=0). Exchange values takes as the last time point. Horizontal dotted line is the theoretical monolayer sorption capacity of hematite based on a surface site density of 2.5 sites nm^{-2}.[17] Dashed line is the percentage of iron atoms located at the surface (See SI for calculation). All reactions contained 2 g Hem L^{-1} buffered at pH 7.5.

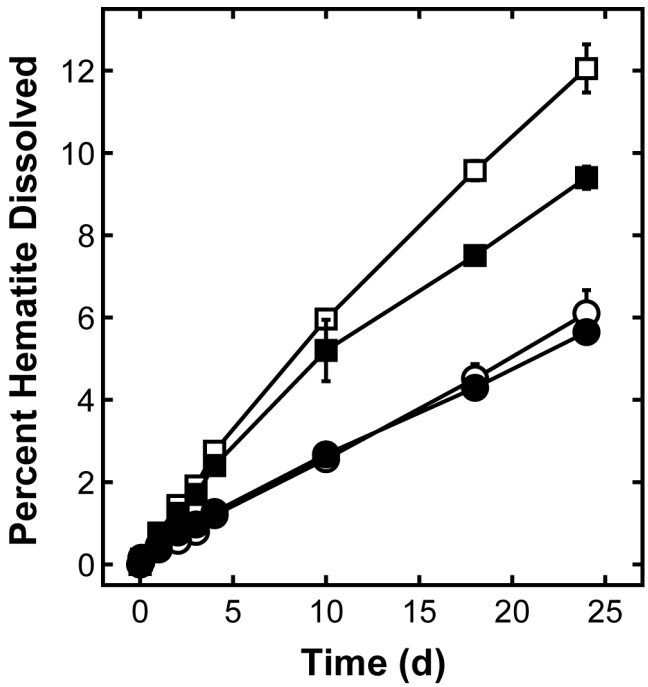

Figure 6. Relative amount of 54 $m^2 g^{-1}$ (**squares**) and 27 $m^2 g^{-1}$ (**circles**) hematite reductively dissolved in 10 mM ascorbic acid (pH 3.1). Hematite solid loading was 0.5 g L^{-1}. Each hematite material was pretreated by reaction in a pH 7.5 buffered fluid in the absence (**open symbols**) and presence of 1 mM $Fe(II)_{aq}$ (**filled symbols**).